



ELSEVIER

Journal of Hazardous Materials 72 (2000) 217–236

**Journal of  
Hazardous  
Materials**

www.elsevier.nl/locate/jhazmat

# Field and numerical analysis of in-situ air sparging: a case study <sup>1</sup>

M.L. Benner <sup>a</sup>, S.M. Stanford <sup>b</sup>, L.S. Lee <sup>c</sup>, R.H. Mohtar <sup>a,\*</sup>

<sup>a</sup> *Agricultural and Biological Engineering Department, Purdue University, West Lafayette, IN, USA*

<sup>b</sup> *Integrated Environmental Solutions, Chesterton, IN, USA*

<sup>c</sup> *Department of Agronomy, Purdue University, West Lafayette, IN, USA*

---

## Abstract

An in-situ air sparging operation was used to remediate the sandy subsurface soils and shallow groundwater under a drum storage site near Chicago, IL, where either periodic or random spillage of a light non-aqueous phase liquid (LNAPL) occurred between 1980 and 1987. Both field measurements and model simulations using commercially available computer software suggested that microbial degradation was the most significant contributor to the removal of contaminant mass. Toluene, ethylbenzene and total xylenes (TEX), which were of major concern with regards to reaching clean-up criteria at the site, were observed to decline by 88% in concentration. Furthermore, up to 97% of the total mass removed through microbial degradation consisted of TEX. Of the total contaminant spill, up to 23% of initial organic chemical mass was removed through microbial degradation compared to less than 6% by physical stripping. Greater loss to microbial degradation is most likely attributed to the relatively low air injection rate used during the course of the air sparging remediation. Evaluation of air sparging at the site using model simulations supported this analysis by estimating 140 and 620 kg of total contaminant mass being removed through volatilization and biodegradation, respectively. An evaluation of several system design parameters using model simulations suggested that only the type of sparging operation (i.e. pulsed or continuous) was significant in terms of total contaminant removal time, while both the sparging operation and air injection rate were significant in terms of removal of a critical species, total xylenes. © 2000 Elsevier Science B.V. All rights reserved.

*Keywords:* In-situ air sparging; Soil vapor collection; Biodegradation; Volatilization; Groundwater remediation

---

\* Corresponding author. Tel.: +1-765-494-1791; fax: +1-765-496-1115; e-mail: mohtar@ecn.purdue.edu

<sup>1</sup> Purdue University Agricultural Research Program Journal number: 16089.

## 1. Introduction

Remediation of contaminated soil and groundwater has become an important issue in recent years. The U.S. EPA, in a 1977 report to congress, stated that at least 17 million waste disposal facilities were placing more than 6.5 billion m<sup>3</sup> of liquid into the ground each year (Freeze and Cherry [1]). Considering underground storage tanks (USTs) alone, the U.S. EPA [2] reported that over 100,000 leaking USTs have been identified in 80 different areas of the nation, thus resulting in significant potential for groundwater contamination. This is especially important when one considers that 51% of the U.S. population utilizes groundwater as a source of drinking water (U.S. EPA [2]). As a result, the search for effective technologies for the remediation of contaminated groundwater has become important.

One such remediation technology, known as in-situ air sparging, has gained a great deal of attention in the past decade. Air sparging can be effective in removing volatile organic compounds (VOCs) from both the vadose and saturated zones of the soil subsurface. The air sparging technique involves forcing air through a point or points at or below the water table. Through the difference in densities between air and water, this injected air will begin an upward migration towards the ground surface, forming a zone of partial desaturation in the saturated zone. As the air rises through the contaminated media, VOCs are stripped and carried to the surface where they may be captured by a soil vapor extraction (SVE) system, commonly used in conjunction with air sparging, for removal and proper treatment of the organic vapors.

In addition to the physical stripping of VOCs, air sparging can enhance aerobic biodegradation processes. Aerobic microbes can use organic chemicals as substrates for energy and growth, converting the organic chemicals into harmless byproducts such as carbon dioxide, cell mass, inorganic salts, and water (Reinhard [3]) so long as nutrients and molecular oxygen are not limiting. The relative contribution between stripping and microbial degradation to organic contaminant removal will be a function of airflow velocity, contaminant volatility (Henry's Law constant), microbial preferences factors, and phase distributions of contaminants. As a result, the design and operation of an air sparging remediation system can significantly affect the dominance of either contaminant stripping or biodegradation at a particular site.

The objectives of the work reported here were to evaluate: (1) the relative contributions of volatilization and microbial degradation at an in-situ air sparging remediation site contaminated through the spillage of a light non-aqueous phase liquid (LNAPL) waste using field measurements and a commercially available computer model; and (2) the relative importance of several system design parameters of the site in terms of contaminant removal time.

## 2. Site and methods description

### 2.1. Site

The site is located in northern Porter County, IN, near the southern shore of Lake Michigan situated at the eastern margin of a large mill complex. Between 1980 and

1987, a small portion of the study area was utilized to store, in 208-l drums, spent non-halogenated solvents containing ink and varnish residues generated from the cleaning and maintenance of tin plate sheet coaters and lithographic presses. The drums were stored in a 20-cm thick slag pavement above ground. The former drum storage area (DSA) measured approximately 12 m by 18 m in plan dimension, and was enclosed by a chain-link fence. The configuration of the former DSA and surrounding study site is illustrated in Fig. 1.

Fig. 2 presents a geological cross-section that illustrates the spatial relationships between stratigraphic units beneath the study area summed from soil borings. Immedi-

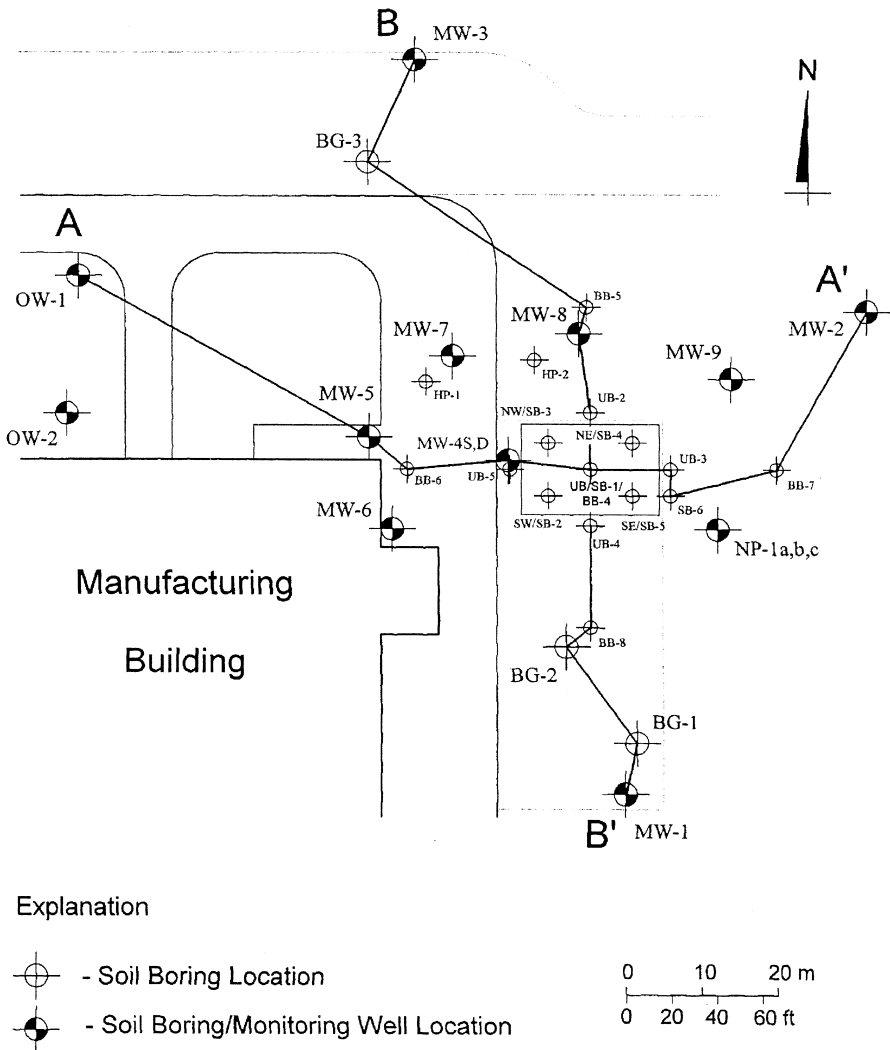


Fig. 1. Former DSA study area layout.

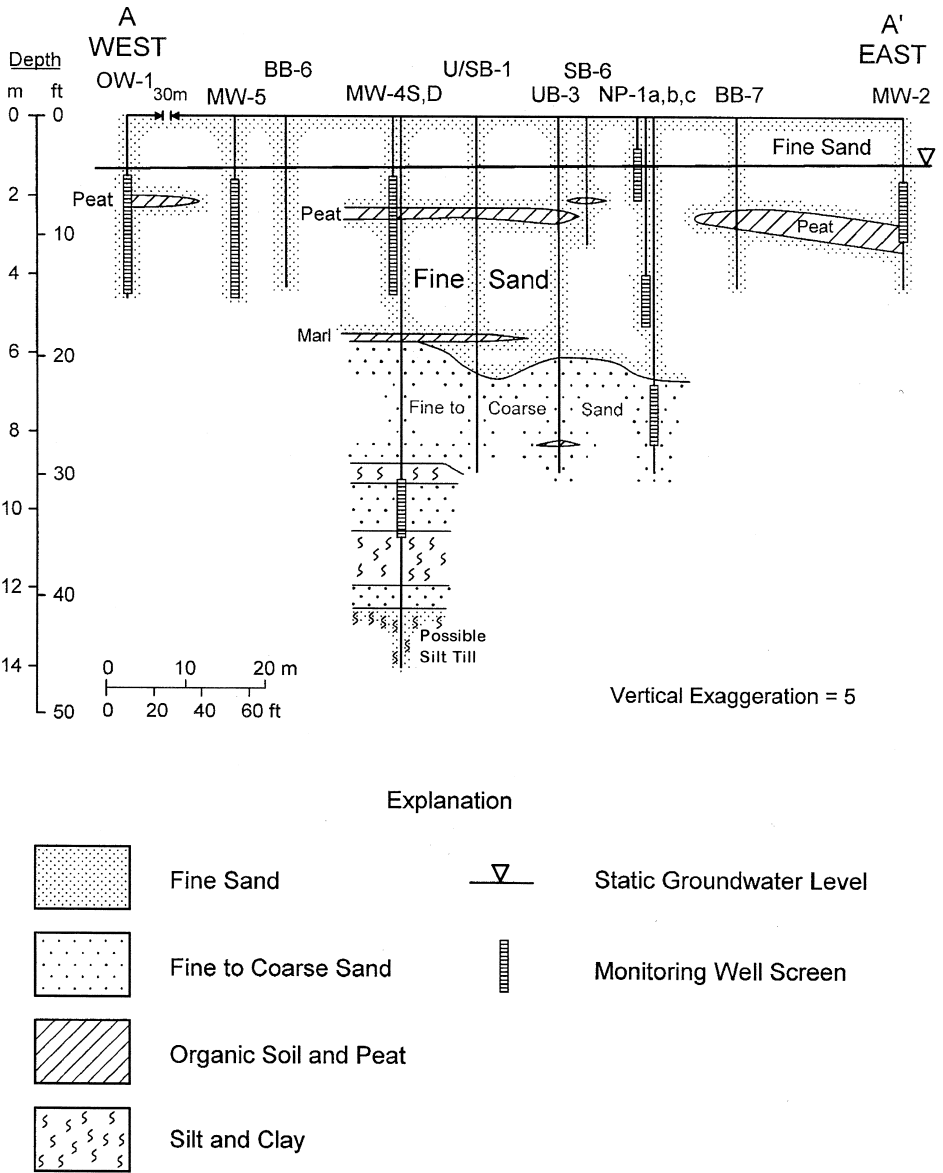


Fig. 2. Soil profile.

ately beneath the surface, which is partly paved and partly covered with sandy topsoil, each boring encountered a layer of well-sorted fine-grained sands extending to some 4.6–5.5 m in depth. This layer is typically interrupted near its midpoint by dark brown to black, fibrous to non-fibrous peats containing varying proportions of fine sand. The next soil layer consists of a 0.3–0.9 m layer of generally gray silty marl often underlain

by 0.3–0.9 m of gray silty fine sand. The above series of sediments is underlain by a second significant layer of sand measuring on the order of 3.0 m in thickness and variable texture ranging between fine and coarse, including some areas with fine gravel. Such textures correspond to materials laid down as washover in the foreshore environment. Only the boring for monitoring well 4 (MW-4D) was advanced to greater depths, revealing a layer consisting largely of silt. Most monitoring wells and piezometers are screened in the uppermost aeolian sands; however, as illustrated in Fig. 2, it is unclear whether MW-4D is screened within overlying sands of the foreshore or within a layer of outwash forming part of the silt till.

Water level vs. time trends indicate an aquifer that is responsive to precipitation and subject to rapid fluctuation between depths of approximately 0.55 and 2.4 m beneath the ground surface. Site-specific potentiometric measurements indicate a generally westerly flow, with gradients ranging between 0.0017 and 0.0063. Average hydraulic conductivities reported for the site range from a minimum of  $8.6 \times 10^{-3}$  cm/s to a maximum of  $6.1 \times 10^{-2}$  cm/s. Using a form of Darcy's Law, average linear groundwater flow velocities are calculated to range between 0.09 and 2.4 m/day.

## 2.2. Contamination

In the former DSA, either periodic or random spillage of an LNAPL occurred between 1980 and 1987. In 1991, the lateral and vertical extent of soil contamination was determined by analyzing several soil borings using extraction and GC/MS techniques in accordance with U.S. EPA Methods 8240 and 8270 (U.S.EPA [4,5]; Stanford [6]). From the soil boring data,  $4600 \pm 2300$  kg of LNAPL, of which  $350 \pm 175$  kg is toluene, ethylbenzene and total xylenes (TEX), were estimated to be present at the site prior to remediation attempts. The primary contaminants, or groups of contaminants, their properties, and average soil concentrations are summarized in Table 1. Contamination was found to be localized and most concentrated in the soils and groundwater directly beneath and directly hydraulically down gradient (west) of the DSA with a maximum estimated area of contamination being  $12 \text{ m} \times 34 \text{ m}$ . Vertical migration was limited to depths no greater than 6.7 m below the ground surface, which corresponds to the fluctuating water table surface or "smear zone."

The lateral and vertical extents of groundwater contamination were determined using monitoring wells and piezometers. The maximum observed lateral extent of organic chemical migration in the groundwater was observed 20 m from the boundary of the DSA in monitoring well MW-5. This distance is considerably less than would be expected based on unretarded conservative transport at the rate of the groundwater's average linear flow velocity. Retardation and biological degradation are believed to have accounted for the observed difference.

The presence of NAPL at the site was determined to exist in at least four locations located directly beneath the DSA (SB-1, SB-2, SB-4, and SB-5, as identified in Fig. 1), using a method detailed by Feenstra et al. [7]. This method requires site-specific estimates of total contaminant soil concentrations, moisture content, porosity, a range of soil organic matter contents, and air, soil, and water equilibrium distribution coefficients available in literature. The presence of an NAPL can be assumed if the hypothetical

Table 1  
Summary of selected contaminant properties and site characterization

Group name	Average molecular weight (g/mol)	Vapor pressure at 20°C (atm)	Aqueous solubility (mg/l)	Kow <sup>a</sup>	Preference factor <sup>b</sup>	Mean concentration (µg/kg)	Total kilogram on site	Mass fraction
Toluene	92	0.029	515	490	490	10,261	19.63	0.0042
Total xylenes ( <i>m, o, p</i> )	106	0.0066	175	589	589	132,667	302.00	0.0646
Trimethylbenzenes	120	0.0032	57	4266	4266	19,199	396.70	0.0849
1,2,3,5-Tetramethylbenzene	134	0.0006	3.5	12,589	12,589	275,133	642.1	0.1373
Ethylbenzene	106	0.0092	180	875	875	15,667	31	0.0066
Ethylmethylbenzenes	120	0.0045	94	4266	4266	61,934	138.3	0.0296
Ethyl dimethyl and ethynyl ethylbenzenes	133	0.0008	21	44,668	44,668	449,407	993.65	0.2125
Propylbenzenes	137	0.002	23	12,589	12,589	115,400	278.90	0.0597
Acidic benzenes	134	0.000014	2594	219	219	63,333	146	0.0312
Naphthalenes	131	0.0001	33	3465	3465	49,423	101.19	0.0216
C8 compounds	112	0.018	5	16,218	16,218	13,267	22.3	0.0048
C9 compounds	126	0.0062	0.15	4.50E+05	4.50E+05	237,500	411.99	0.0881
C10 compounds	142	0.0018	0.015	1.78E+06	1.78E+06	281,767	546.51	0.1169
C11–13 compounds	157	0.0006	0.015	1.10E+06	1.10E+06	291,286	644.65	0.1379

<sup>a</sup>Octanol–water distribution coefficient.

<sup>b</sup>Biological preference utilization factor describing the preferential degradation of certain contaminants over others. Experimental evidence suggests that this factor can be reasonably estimated by the Kow of the species (ES&T [11]).

maximum total soil concentration defined by the solubility of the chemical in water, the saturated soil gas concentration, and the sorption capacity of the soil solids is exceeded. Furthermore, droplets of LNAPL were observed from time to time in the purge water collected during sampling in monitoring well MW-4S, located at the westerly margin of the DSA.

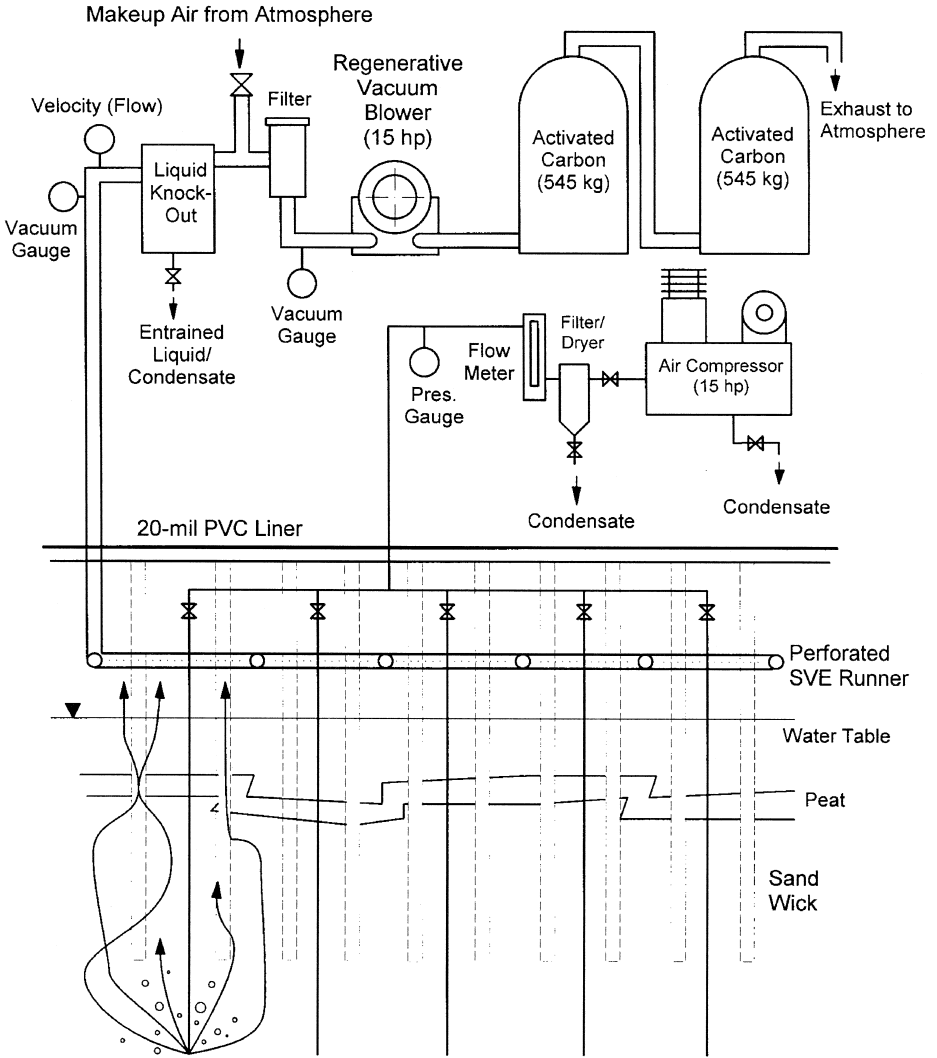
### 2.3. Remediation criteria

Site closure and clean-up criteria were set by the Indiana Department of Environmental Management (IDEM) under its authorization to implement the Resource Conservation and Recovery Act (RCRA) program as delegated by the U.S. EPA. At this particular facility, clean-up criteria for anthropogenic organic chemicals in the top 0.61 m of soil and in the groundwater were set at their practical quantitation limits (PQLs). For groundwater, two types of criteria were established. Reduction in concentration to federally enforceable drinking water standards or maximum contaminant levels (MCLs) for chemicals regulated under such a standard was considered acceptable. For chemical of interest in groundwater with no MCL and for all soil concentrations, the PQL for each chemical was considered acceptable. PQLs are 5–10 times greater than the lowest limit of analytical detection, which is matrix-specific, and the primary chemicals of interest at this site include all aromatic compounds listed in Table 1. For groundwater criteria defined by PQLs, criteria must not be exceeded for two consecutive quarters. At one point in the sparging operation, it was thought that all clean-up criteria had been achieved, but naphthalene concentrations exceeded the PQLs for two consecutive samplings, at which time remediation operations were reinitiated. Subsurface soil concentrations were not regulated directly; however, note that groundwater concentrations, which are a function of subsurface soil concentration, were monitored and regulated.

### 2.4. Remediation system

In-situ air sparging was implemented to remediate the contamination beneath the DSA. To minimize atmospheric discharge of organic chemicals, air sparging was augmented with a soil vapor collection system. Operation of both the air sparging and soil vapor collection systems was initiated in October 1992 and concluded 3 years later in October 1995. Due to the reoccurrence of several compounds in groundwater beneath the site, the remediation system was restarted in early March 1997 until late July 1997, when the compounds of interest were detected below concentrations of concern.

A cross-sectional schematic of the remediation system used at the DSA is illustrated in Fig. 3. The air sparging system was constructed to include the installation of 10 equally spaced air injection wells of which six were located within the boundary of the DSA and four immediately to the west to address down gradient subsurface migration. Each air injection well was completed to depths of approximately 6.1 m and terminated with a no. 20-slot well screen measuring approximately 0.30 m in length. The well casings (0.108 m i.d.) and screens were constructed of ASTM schedule 40 PVC. Air was supplied by a 15-hp reciprocating piston type air compressor, conditioned using a



Example of Upward Path of Injected Air for Each Well

Fig. 3. Schematic representation of air sparging and soil vapor collection system showing system components and control scheme.

combination filter/dryer, and routed through a variable-area bypass flow meter prior to distribution. In addition to air injection wells, approximately 36 sand wicks were placed in areas around and between the injection wells to minimize the potential for forced lateral migration of air which might become trapped beneath the soil layers of low conductivity. The sand wicks consisted of soil borings constructed to depths of approximately 2.4–3.1 m each and back-filled with well-graded construction sand. Their use,



which was intended to “engineer in” a degree of homogeneity in a heterogeneous subsurface, most likely caused some unknown degree of preferential flow through the wicks, thus affecting stripping efficiency in the system.

The soil vapor collection system consisted of a series of linked horizontal runners buried at a depth of approximately 0.91 m and arranged in a multi-cellular rectangular pattern surrounding each air injection well. Overlying areas that were not paved with asphaltic concrete were covered with a 20% PVC membrane to reduce the potential for short-circuiting. In operation, a vacuum was applied to the vapor collection runners using a 15-hp regenerative vacuum blower that was capable of drawing air at a rate of 6.0 standard cubic meter per minute (scmm) at a maximum vacuum load of 254 cm of water.

The air sparging system was operated to provide between 0.35 and 0.51 scmm of air equally distributed among the 10 injection wells, and under pressures of approximately 9.1–14.1 m of water as measured in the remediation system shed. The soil vapor collection system was operated at vacuums ranging between 7.6 and 100 cm of water, with control being accomplished with the introduction of makeup air. The flow of vapor yielded by the subsurface was monitored by measuring the velocity of the piped air stream and calculated as the product of the velocity and the cross-sectional area of the pipe. During remediation, air injection and vapor collection were essentially continuous with the exception of occasional shutdowns due to mechanical difficulties. Based on weekly measurements of the air injection rate, a total of approximately 620,000 standard cubic meter (scm) of air were injected by the air sparging system and approximately 1,600,000 scm of air were withdrawn by the soil vapor collection system. Good recovery of injected air is suggested since the volume extracted was larger than the volume injected, particularly early in the remediation process.

In addition to monitoring the volume of air removed, soil vapors were periodically tested for VOCs using a photoionization detector (PID) and for CO<sub>2</sub> using short-term detector tubes. Assuming ideal gas behavior and an average molecular weight for the VOCs of 106.2 g/mol, concentrations derived from the PID were converted to cumulative mass using flow rates determined weekly. Likewise, CO<sub>2</sub> concentrations were converted to mass and corrected for ambient CO<sub>2</sub> concentrations. Water in the monitoring wells was assayed for pH, specific conductance, temperature, VOCs, semi-volatile organic compounds (SVOCs) and dissolved oxygen (Stanford [6]).

### 2.5. Modeling design and calibration

Numerical modeling of in-situ air sparging at the DSA study area was performed using BIOVENTING<sup>plus</sup>, a commercially available software model developed by Environmental Systems and Technologies (ES & T [8]). BIOVENTING<sup>plus</sup> is aimed to aid in the design of remediation technologies for soil and groundwater contaminated with organic chemicals. Many processes relevant to in-situ air sparging have been incorporated in the software such as multi-directional airflow, multiphase and multi-component chemical partitioning, velocity-dependent vapor stripping, and nutrient-limited, oxygen-limited or mass transfer-limited biodecay.

The model operates by first calculating the air flow and air pressure distribution around each sparging well using the DeGlee–Hantush–Jacob solution (Bouwer [9]) with

adjustments considered for soil capillary head pressure and water saturation. Following this, mass removal is calculated using a finite difference approach that considers vapor recovery, biodecay and free product removal as:

$$\frac{-dM_i^j}{dt} = J_{V_i}^j + J_{B_i}^j + J_{F_i}^j, \quad (1)$$

where  $M_i^j$  is the mole of species  $i$  in cell  $j$ ;  $t$  is time; and  $J_{V_i}^j$ ,  $J_{B_i}^j$  and  $J_{F_i}^j$  are the rates of component loss due to vapor recovery, biodecay and free product removal, respectively, within cell  $j$  (ES & T [8]).

The vapor removal term considers equilibrium molar gas concentrations, airflow rate, and a non-equilibrium efficiency factor dependent on adjusted input parameters known as the turnover time for 50% efficiency ( $T_{50}$ ) and off-cycle time for  $2 \times$  efficiency (OCT) as shown in Eqs. (2a) and (2b):

$$E_s = \frac{1}{1 + T_{50}P}, \quad (2a)$$

$$E_{\max} = 1 - (1 - E_s) \exp\left(\frac{-0.69t_{\text{off}}}{\text{OCT}}\right), \quad (2b)$$

where  $E_s$  is a steady-state efficiency factor,  $P$  is the pore volume turnover rate (pore volumes per time),  $E_{\max}$  is an efficiency factor representative of the onset of a pulsed sparging cycle, and  $t_{\text{off}}$  is the off-cycle duration (ES & T [8]). The biodecay term of Eq. (1) considers either oxygen-limited biodecay, dissolution-limited biodecay or a specified maximum biodecay, all of which are dependent on a preference factor specific to each species of contaminant relating to the preferential utilization of that species by the microbial population. Experimental evidence suggests that substrate uptake (being organic contaminants) by microbes is species-dependent, being smaller for more soluble aromatics and larger for less soluble alkanes. The preference factor allows for the model to compensate for this. Although its effects on an estimated time to reach a specified remediation goal can be significant, design optimization does not appear to be affected (ES & T [11]).

The final term of Eq. (1), free product removal, considers the physical removal of liquid phase product and is not associated with air sparging. It is difficult to simulate simultaneous air sparging and SVE using BIOVENTING<sup>plus</sup>; therefore, only in-situ air sparging was modeled. This is justified in that, at the DSA study area, the SVE system served only as a vapor collection system and did not significantly enhance contaminant removal; therefore, modeling site operations assuming only air sparging should be adequate. Modeling was performed by inputting known values (measured at the site) for as many of the model's input parameters as possible. Those values not measured at the study area were estimated based on reasonable values found in the literature as noted in Table 2. The input format of the contaminant composition was primarily represented in compound groups as shown in Table 1 because properties for many of the individual contaminants at the study area are not explicitly known. Calibration for the horizontal air conductivity and anisotropy ratio (the ratio of horizontal to vertical permeability) parameters was performed by matching simulation results for the sparging air pressure

Table 2  
Model input values for the DSA study area

Parameters	Model input
Air conductivity	129.6 m/day <sup>a</sup>
Anisotropy ratio	2.6 <sup>a</sup>
Porosity	0.3 <sup>b</sup>
Pore size distribution coefficient	2.3 <sup>c</sup>
Organic carbon content	0.006 <sup>a</sup>
Maximum biodecay rate	0.34 mg kg <sup>-1</sup> day <sup>-1d</sup>
Aquifer temperature	15°C <sup>c</sup>
Turnover time for 50% efficiency	2.59 days <sup>a</sup>
Off-cycle time for 2× efficiency	1.00 day <sup>a</sup>
Contaminant type	Table 1
Contaminated soil area	408 m <sup>2b</sup>
Total contaminant mass	4600 kg <sup>b</sup>
Total contaminated soil volume	883 m <sup>3b</sup>
Remediation system	Air sparging
Depth of sparge point below water table	4.11 m <sup>b</sup>
Well diameter including filter pack	0.108 m <sup>b</sup>
Air injection rate	0.0434 m <sup>3</sup> /min <sup>b</sup>
Air injection pressure	0.88–1.4 atm <sup>b</sup>
Number of wells	10 <sup>b</sup>
Sparging operation	continuous <sup>b</sup>
Duration of sparging	1113 days <sup>b</sup>

<sup>a</sup>Calibrated/adjusted value.

<sup>b</sup>Field measurement.

<sup>c</sup>ES&T [8].

<sup>d</sup>Estimated from field data.

and radius of influence to those reported at the site. Adjustment of the  $T_{50}$  parameter was performed by matching simulation results for off-gas concentration at time zero and total contaminant removal through volatilization to those measured in the field. While the sand wicks used at the site could not be directly incorporated into the site modeling, their effect on contaminant removal was indirectly incorporated into the choice of the  $T_{50}$  parameter.

Although air pressure and volatilized contaminant mass are known, measurements of the radius of influence and off-gas concentration were not. As a result, a radius of influence of 4.42 m was estimated assuming uniformity between radii of influence and based on the known width of contamination, 34 m, the number of wells covering that width, five wells, and assuming a 30% overlap. A concentration range of 0–0.455 mg/l was made based on off-gas measurements taken at the end of the first week of operation. While the radius of influence may be slightly overpredicted, later analysis shows that above a coverage where adjacent radii of influence just touch, little effect on contaminant removal is observed.

As a result of these site estimates, the horizontal air conductivity, anisotropy ratio and  $T_{50}$  input parameters were adjusted to their final values shown in Table 2. Importantly, this calibration considered the recovery of total petroleum hydrocarbons (TPH) and not

the recovery of any singular species that may be of interest with regards to specific clean-up criteria at the site. Furthermore, to obtain a more accurate adjustment of the  $T_{50}$  parameter, mass removal results were used for volatilization only instead of combined volatilization and microbial degradation, as measurements of volatilized mass were the most accurately measured.

### 3. Contaminant removal assessment

#### 3.1. Field results

By conducting a mass balance with the assumption that equilibrium is achieved, it is possible to understand the partitioning between contaminant removal due to air stripping and biological degradation at the DSA. The mass of contaminant removed by volatilization is estimated by monitoring the soil vapor system exhaust. The mass of contaminant biologically degraded is estimated from equations such as that for the aerobic degradation of toluene shown below:



assuming that the mass of the carbon dioxide reaction product is known.

After approximately 3 years of sparging at the DSA study area, all chemicals of concern had reached their respective clean-up criteria, as specified by IDEM, and the system was shut down. Following three consecutive quarters of post-remediation monitoring, low levels of naphthalene reappeared in monitoring well MW-4S. Furthermore, low levels of 2,4-dimethylphenol and 4-methylphenol also appeared for the first time, thus requiring the remediation system to be restarted for approximately 5 months until all three of these compounds were again absent. Monitoring continued for approximately three quarters following that time.

While contaminants at the site reached their respective clean-up criteria, the mass removed through volatilization was surprisingly small. Based on weekly field PID measurements, the best estimates suggest that only 1–2 kg of TEX and between approximately 20 and 140 kg of total contaminants were removed through volatilization. This estimated range includes a single, exceedingly high PID measurement obtained during the second week of operation that accounted for approximately 120 kg of the total recovered. While the measurement itself is reasonably accurate, its use in the calculation of recovered contaminant mass during that week may have resulted in an overestimation. Nonetheless, considering the upper bound value of 140 kg, no more than approximately 6% of the total initial contaminant mass was removed through volatilization during air sparging. During the design phase, it was expected that volatilization and subsequent stripping would remove a much larger quantity of contaminants, thus the vapor collection system included 1090 kg of ground activated carbon for control of atmospheric emissions. The small proportion of total contaminant mass removed by physical processes is most likely due to the relatively coarse channeling of airflow through the saturated zone, perhaps induced by the presence of the sand wicks. A relatively wide spacing between air channels would decrease the efficiency of air

stripping due to diffusion-limited mass removal. Furthermore, the low air injection rates employed at the study area are conducive to yielding low efficiencies in volatilization of contaminant mass.

Measurements of dissolved oxygen concentrations in the groundwater beneath the study area indicated that during air sparging, the groundwater was in an aerobic condition. Therefore, when viewed in terms of the 1800 kg of CO<sub>2</sub> yielded by the soil vapor collection system during air sparging, the stoichiometry of Eq. (3) is consistent with the complete aerobic mineralization of approximately 540 kg of the organic contaminants. A reaction to this extent would imply the utilization of approximately 1700 kg of molecular oxygen, or 1% of what was injected. This implies an oxygen transfer efficiency between the injected air and groundwater of approximately 1%.

TEX concentrations declined by 88% during air sparging and their molar proportion in the LNAPL phase declined by the same amount. Considering that the initial mass of TEX was 350 ± 175 kg, and that only 1–2 kg of TEX were volatilized, between 30% and 97% of biologically degraded mass must have consisted of TEX. This implies that TEX was degraded with a mass preference of at least 3:1 relative to the other hydrocarbons that were present in the subsurface. This also shows that a significant amount of the total contaminant mass removed at the site consisted of TEX compounds, all of which were of special concern in terms of addressing clean-up criteria.

Based on field estimates, approximately 560–680 kg of total contaminant mass were removed during air sparging through both volatilization and microbial degradation processes. This results in between 1620 and 6340 kg of total contaminant remaining at the site. Although this is a large amount of contaminant mass, which may result in a future groundwater concentration rebound, the clean-up criteria established by IDEM for the contaminant concentrations in groundwater were met, thus allowing site closure. IDEM did not impose clean-up criteria for the subsurface soils.

### 3.2. Model results

The effects of volatilization and microbial degradation on total product hydrocarbon (TPH) removal and the removal of selected species at the study area were addressed using BIOVENTING<sup>plus</sup>. As previously described, model calibration was performed, in part, by assuming no biodegradation in the field. As a consequence, results from this simulation describe volatilization (vapor removal) only. A further simulation was performed including biodecay using a field data estimate of the maximum biodecay rate, thus allowing for a determination of TPH mass removal by each mechanism to be made. It is important to note that these simulations assumed an initial TPH mass of 4600 kg and considered removal processes for the entire contaminant mass present at the site and not the mass of contaminants important in terms of the site clean-up criteria.

As shown in Fig. 4, the first simulation (addressing volatilization only) calculated that 140 kg of TPH were removed during 1113 days of sparging at the study area. As expected, this calculation matches well with the upper estimate of removal through volatilization reported at the study area. The second simulation, also shown in Fig. 4 (addressing both volatilization and biodegradation), calculated that 760 kg of TPH were

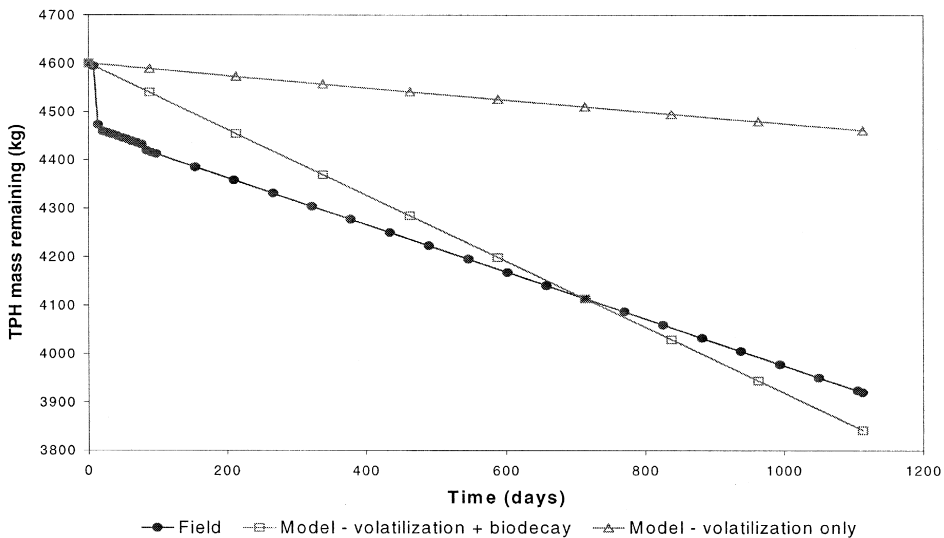


Fig. 4. Field and simulation results for total contaminant mass remaining vs. time.

removed during the course of sparging, leading to an estimate of 620 kg of TPH removed through biodegradation alone. Relative to field measurements, model simulations predicted approximately 11.5% more TPH removal through volatilization and 14.6% more TPH removal through biodegradation; however, model and field results were considered reasonably accurate (Benner [10]).

To gain a better understanding of which species within the entire contaminant spill were preferentially removed and how site closure was obtained despite the large amount of total contaminant mass remaining, data for TEX and naphthalene were extracted from the previously mentioned simulations. Of these solutes, only toluene was volatilized to a greater proportion than what was biodegraded (Fig. 5), likely due to its high volatility (large Henry's Law constant) and low microbial preference factor as compared to the other three species. Furthermore, results for TEX removal through volatilization and biodegradation indicate removal of approximately 35 and 38 kg, respectively, with a total TEX removal of 73 kg. While these results are considerably different than those obtained in the field, the error most likely occurs from the fact that model calibration was performed for the entire contaminant spill and not for this individual subset of species important to the site in terms of clean-up criteria. Simulated results also show that, relative to the initial mass of each species, 43% of toluene, 25% of ethylbenzene, 19% of total xylenes, and 10% of naphthalene were removed. The percentage removed is directly proportional to the reduction in groundwater concentrations observed at the site, leading to site closure although a large mass of contaminant persisted in the subsurface following remediation. Despite the discrepancy in results, the model's analysis of the study area supports the field analysis that biodegradation played the most significant role in contaminant removal. As previously mentioned, for both field and

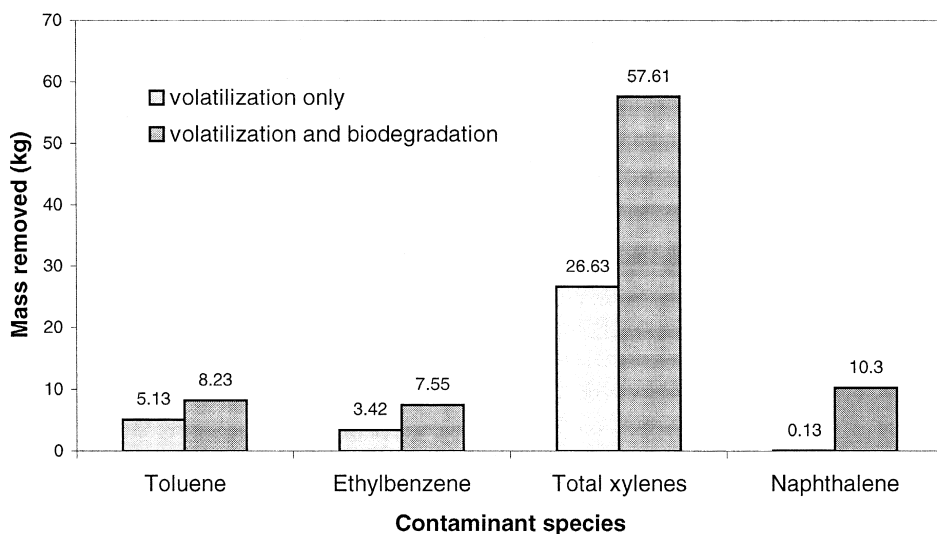


Fig. 5. Simulation results for individual contaminant mass removed.

simulation results, microbial degradation caused the removal of a far greater amount of contaminant than did volatilization.

#### 4. Evaluation of system design parameters

Evaluation of several air sparging system design parameters was conducted using BIOVENTING<sup>plus</sup>. Model simulations were performed to evaluate the significance of the following system design parameters in terms of total contaminant removal: (1) air injection rate, (2) number of air sparging wells used, (3) depth of the sparging point below the water table, and (4) pulsed vs. continuous sparging operation. Simulations were performed by testing values for each of the four system design parameters ranging from  $-100\%$  to, in some cases,  $+800\%$  of the original “base case” value reported at the field. Furthermore, to gain a better understanding of the overall significance of each parameter, simulations were run to test each parameter in terms of TPH removal and the removal of total xylenes (a contaminant species of significant importance at the site). The latter aids in “factoring out” each parameter’s effects on a critical species which would otherwise be lost when looking only at the removal of the entire contaminant spill.

Three simulations were performed using varying clean-up criteria; (1) TPH concentration = 50 mg/l using the calibrated value of  $T_{50}$  (2.59 days) or OCT (10 days); (2) total xylenes concentration = 10 mg/l using the calibrated value of  $T_{50}$  or OCT; and (3) total xylenes concentration = 10 mg/l using  $T_{50} = 1$  day or OCT = 1 day. The various  $T_{50}$  values were used for simulations involving the air injection rate, number of wells, and depth of the sparging point parameters. For the pulsed sparging parameter, the

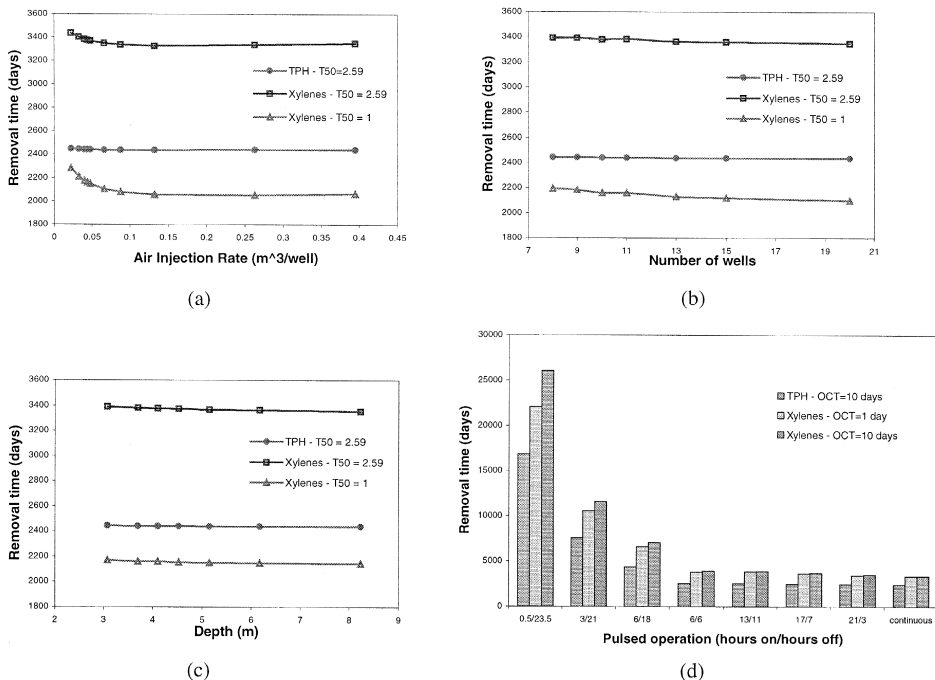


Fig. 6. System design parameter evaluation results for (a) air injection rate, (b) number of wells, (c) depth of the sparging point below the water table, and (d) pulsed sparging operation.

various OCT values were used due to this parameter's more direct influence on pulsed sparging operations. While OCT was not directly calibrated, as was  $T_{50}$ , an abbreviated sensitivity analysis showed a value of 10 days to be reasonable. For each parameter, results for the first simulation were reported in terms of removal time needed to reach the TPH clean-up criteria, while results for the second and third simulations were reported in terms of removal time needed to reach the total xylenes removal criteria. Furthermore, the third simulation involved using a lower value of  $T_{50}$  or OCT, which acts to represent the increased removal efficiency most likely seen with this type of contaminant (Benner [10]).

#### 4.1. Air injection rate per well

Rates of air injection were varied from  $-100\%$  to  $+800\%$  from the original  $0.0439$  scmm used at the site. As seen in Fig. 6a, removal times for TPH varied less than  $1\%$  with minimum and maximum values of 2437 and 2448 days, respectively. Removal times for total xylenes ( $T_{50} = 2.59$  days) varied by approximately  $3\%$ , with minimum and maximum values of 3329 and 3437 days, respectively. Removal times for total xylenes ( $T_{50} = 1$  day) varied by approximately  $11\%$ , with minimum and maximum values of 2055 and 2283 days, respectively.

The lack of significance of air injection rate in terms of TPH removal is likely attributable to the semi-volatile nature of the contaminant spill as a whole and the



dominance of microbial degradation at the study area. As a result, higher injection rates will not significantly enhance the overall stripping process; therefore, as long as a sufficient amount of oxygen is injected into the subsurface, microbial activity will be enhanced and act as the dominant removal mechanism. The significance of air injection rate increases with regard to the removal of total xylenes due to their larger volatility and lower microbial preference compared to the contaminant average in the NAPL as represented by TPH. Consequently, variations in air injection rate will have greater effects on removal through volatilization as opposed to biodegradation, therefore causing larger variations in removal times. This phenomenon is most evident in the simulations involving a  $T_{50}$  of 1 day which, as previously mentioned, more accurately models the system's removal efficiency of total xylenes.

The slight trends of decreasing and then increasing removal time seen in Fig. 6a are likely a consequence of several processes. As air injection rate increases from 0.022 to 0.044 scmm, pore volume turnover rates increase, causing enhanced volatilization at the expense of only a minor reduction in biodegradation, thereby decreasing the overall removal time slightly. At injection rates above 0.044 cfm, airflow velocity becomes more detrimental to microbial activity while the residence time of the injected air begins to increase beyond a time reasonable for proper volatilization. As a result, a slight increase in removal time is observed.

#### 4.2. Number of wells

The number of wells was varied from 8 to 20 wells relative to the 10 wells actually employed at the site. Shown in Fig. 6b, removal times for TPH decreased from a maximum of 2443 days for eight wells to a minimum of 2436 days for 20 wells. Removal times for total xylenes decreased from 3394 days (eight wells) to 3351 days (20 wells) for  $T_{50} = 2.59$  days and from 2193 days (eight wells) to 2100 days (20 wells) for  $T_{50} = 1$  day. Due to the minor decrease in removal time (4% or less) for a significant increase in the number of wells, this system design parameter does not appear to be significant in terms of either TPH or total xylenes removal at the study area over the range of wells simulated.

This slight decrease in removal time with an increasing number of wells is likely due to improved coverage of “dead zone” areas lying between adjacent wells. In these “dead zones”, air sparging removal efficiencies are minimal, and contaminant removal mechanisms are restricted to natural attenuation and diffusion-limited mass transport to the surrounding air sparging zones of influence. Therefore, as more wells are added to the system, greater overlap will occur between adjacent wells resulting in a decrease in “dead zones” and enhanced contaminant removal efficiency, mainly through volatilization. The slightly larger variations in removal time seen with total xylenes are likely attributable to the greater relative ease of remediation of this contaminant group compared to the entire spill. Due to the size of the sparging well radius of influence and the extent of contamination at the site, BIOVENTING<sup>plus</sup> restricts the number of wells to no less than eight; however, it is expected that with fewer wells, both volatilization and microbial degradation processes will be significantly restricted due to limited airflow coverage, leading to large increases in both TPH and total xylenes removal times.

#### 4.3. Depth of sparge point below water table

Depth of the sparge point below the water table was varied from 3.08 to 8.23 m compared to the original 4.11 m reported at the site. Removal times for TPH decreased from a maximum of 2443 days for 3.08 m below the water table to a minimum of 2437 days for 8.23 m below the water table as shown in Fig. 6c. Removal times for total xylenes decreased from 3391 (3.08 m) to 3355 days (8.23 m) for  $T_{50} = 2.59$  days and from 2173 (3.08 m) to 2145 days (8.23 m) for  $T_{50} = 1$  day. With variations of only 1% or less for a large variation in sparging depth, this system design parameter does not appear significant in terms of either TPH or total xylenes removal at the study area.

The slight decrease in removal time resulting from an increase in the sparging depth is likely due to improved coverage of “dead zones” occurring between adjacent wells, similar to the effect of increasing the number of wells. As depth of the sparge point below the water table is increased, the lateral migration of air will also increase, resulting in a larger radius of influence for each well, provided that the sparging air pressure exceeds the displacement head of the soil matrix. With the larger coverage area resultant from a bigger radius of influence, “dead zones” will be diminished and overall contaminant removal efficiency will be enhanced.

#### 4.4. Pulsed vs. continuous operation

Simulated pulsed sparging operations ranging from on/off times (hours) of 0.5/23.5 were compared to continuous operation. As shown in Fig. 6d, simulations indicated substantial differences in removal times for each sparging operation for both TPH and total xylenes. Furthermore, minimum and maximum values for the various TPH and total xylenes simulations varied by 486% to 783%, leading to the conclusion that this system design parameter was significant at the study area in terms of the total contaminant profile, and also for single species within the profile.

For each of the three simulation sets shown in Fig. 6d, results show that, as pulsed sparging approached continuous operation (i.e. the ratio of time on:time off increased), removal times decreased. On the contrary, as pulsed sparging diverged from continuous operation (i.e. the ratio of time on:time off decreased), removal times increased dramatically. Although pulsed operation allows more time for NAPL dissolution and contaminant desorption from soil, simulations results suggest that mass-transfer constraints were minimal for the contaminant soil site combination investigated. Therefore, the lower removal efficiency observed with increasing off-cycle times was most likely due to a quick depletion of available oxygen through biodegradation of released contaminants during off-cycles. In the absence of mass-transfer constraints, continuous operation results in greater contaminant stripping through volatilization and optimizes oxygen availability, thus contaminant biodegradation.

### 5. Conclusions

This case study illustrates the successful remediation of the DSA study area through in-situ air sparging and the subsequent evaluation of several remediation system design

parameters through numerical modeling. Contamination of soil and groundwater from spillage of 2300–6900 kg of LNAPL was remediated through air sparging-enhanced volatilization and biodegradation. Based on weekly PID measurements, volatilization was reported to have removed approximately 1–2 kg of TEX compounds and between 20 and 140 kg (0.2–6%) of total contaminants at the study area. Through the mass of CO<sub>2</sub> yielded by the study area during air sparging, microbial degradation of contaminants is consistent with the complete aerobic mineralization of approximately 540 kg (8 to 23%) of the organic contaminants. Numerical modeling of total contaminant removal through volatilization and biodegradation was consistent with field results. Although the magnitudes of field and model results were somewhat different, simulations indicated that biodegradation had the largest contribution to total contaminant removal at the site.

Evaluation of several system design parameters used at the study area showed that only the sparging operation (pulsed or continuous) was significant in terms of TPH removal time and that both the air injection rate and the sparging operation parameters were significant in terms of the removal time for total xylenes. This leads to the direct conclusion that different portions of the entire contaminant spill are remediated in distinct ways. It further indicates that the remediation system design should be based on the contaminant species of critical importance and not necessarily the entire contaminant profile. Analyses presented can aid in identifying the system design parameters of greatest importance in meeting site clean-up criteria based on either all or a select group of contaminants, thus streamlining efforts with regards to system optimization.

## Acknowledgements

The authors would like to thank the Agricultural Research Service of Purdue University for their partial funding of this research and Dr. Jack Parker and Mesbah Islam of Environmental Systems and Technologies, Blacksburg, VA, for their assistance and insight. Special thanks also go to Integrated Environmental Solutions, of Chesterton, IN and its partners for their support and assistance.

## References

- [1] R.A. Freeze, J.A. Cherry, *Groundwater*, Prentice-Hall, Englewood Cliffs, NJ, 1979, 604 pp.
- [2] U.S. EPA, National water quality inventory, 1996 Report to Congress, EPA841-R-97-008, Washington, DC.
- [3] M. Reinhard, in: R.D. Norris, et al. (Eds.), *Handbook of Bioremediation, In-Situ Bioremediation Technologies for Petroleum-Derived Hydrocarbons Based on Alternate Electron Acceptors (Other Than Molecular Oxygen)*, Robert S. Kerr Environmental Research Laboratory, CRC Press, Boca Raton, FL, 1994, pp. 131–147.
- [4] U.S. EPA, SW-846 Method 8240A: Volatile Organics by Gas Chromatography/Mass Spectrometry (GC/MS), Vol. 1, U.S. EPA, Washington, DC, 1986.
- [5] U.S. EPA, SW-846 Method 8270A: Semivolatile Organic Compounds by Gas Chromatography/Mass Spectrometry (GC/MS): Capillary Column Technique, Vol. 1, U.S. EPA, Washington, DC, 1986.
- [6] S.M. Stanford, Physical and biological effects of in-situ air sparging of groundwater contaminated with organic chemicals, MS thesis, Purdue University, May 1998.

- [7] S. Feenstra, D.M. MacKay, J.A. Cherry, A method for assessing residual NAPL based on organic chemical concentrations in soil samples, *Groundwater Monitoring Review* (Spring 1991).
- [8] ES&T, BIOVENTING<sup>plus</sup> User and Technical Guide, Version 4.0, Environmental Systems and Technologies, Blacksburg, VA, 1998.
- [9] H. Bouwer, *Groundwater Hydrology*, McGraw-Hill, New York, 1978, pp. 100–103.
- [10] M.L. Benner, Field and numerical analysis of parameters affecting the performance of air sparging remediation systems, MS thesis, Purdue University, May 1999.
- [11] ES&T, BIOVENTING<sup>plus</sup> Version 4: Advances in Modeling Forced Air Remediation, Environmental Systems and Technologies, Blacksburg, VA, 1998.